

Laminar-Turbulent Transition in Stratified Wakes

Patrice Meunier

Abstract This chapter presents experimental and theoretical results on the transition from a laminar to a turbulent wake in a stratified fluid. The case of a cylinder is analysed in detail at low Reynolds number since it gives rise to the famous von Karman vortex street when the Reynolds number exceeds a critical value. This value highly depends on the stratification and on the tilt angle of the cylinder. A moderate stratification tends to suppress the von Karman vortex street, in agreement with the stabilisation of shear flows at high Richardson numbers. However, it is surprising to see that a strong stratification destabilises the flow when the cylinder is tilted. This new von Karman vortex street is allowed because the vortices exhibit horizontal streamlines although the vortices are tilted. The experimental stability diagram obtained by dye visualisations are compared to numerical results. At larger Reynolds numbers, the 2D von Karman vortex street leads to a 3D instability. Shadowgraph visualisations clearly reveal that the unstable mode is similar to the mode A well known in homogeneous cylinder wakes if the cylinder is vertical. This mode seems to be more unstable for moderate stratifications and more stable for strong stratifications. When the cylinder is tilted a new unstable mode appears at moderate Froude numbers, which exhibits thin undulated dark lines. This mode is due to a Kelvin-Helmholtz instability of the critical layer which appears in each tilted vortex of the von Karman street. Finally, at high Reynolds numbers, the wake becomes turbulent in the early stages for the case of a sphere. However, the late stages of the wake exhibit once again a von Karman street of flat horizontal vortices. The size and the velocity of the wake vary algebraically with time. These scaling laws can be predicted by a simple model of turbulent diffusion in the horizontal direction and of viscous diffusion in the vertical direction.

P. Meunier (✉)

Institut de Recherche sur les Phénomènes Hors Equilibre, UMR 6594, CNRS - Aix-Marseille Université, 49 rue F. Joliot Curie, Marseille Cédex 1313384, France
e-mail: meunier@irphe.univ-mrs.fr

1 Introduction

Despite an extensive number of studies on bluff body wakes in a homogeneous fluid, there has been very few results on wakes in a stratified fluid. The goal of this chapter is to analyse the influence of the stratification on the transition from a laminar to a turbulent wake of a bluff body.

Bluff body wakes have been a main subject of interest for engineers due to their application to terrestrial and naval vehicles, where drag reduction has been a major concern for cars, trains and boats. Bluff body wakes have also direct engineering significance for civil constructions, where the presence of alternate vortices in the wakes may cause structural vibrations, acoustic noise and even resonances, leading to catastrophic failures. Of course, the behaviour of the wake is dependent on the shape of the bluff body. However, both boundary layer separation and shedded vortices are present in the wake of a circular cylinder. This basic geometry is thus often used for fundamental studies on bluff body wakes.

The presence of a continuous stratification is characteristic of geophysical applications, since the atmosphere and oceans are stratified in density. This may have an influence on the large scale wakes of mountains and islands but also on the small scale wakes of submarines and off-shore platforms. How much mixing is caused by islands wakes in oceans? Can meteorological weather forecast simulations take into account mountain wakes? Are submarine wakes detectable? Can the off-shore platforms resist in strong storms and currents? All these questions partly motivate this study which however remains very fundamental.

2 Presentation of the Problem

The experimental set-up for the study of the stratified wake of a cylinder is presented schematically in Fig. 1. The experiments are performed in a 150 cm long, 75 cm wide and 50 cm high Plexiglas tank allowing visualisations from all sides. The tank is filled with a linearly stratified fluid up to a height $Z = 45$ cm. The density profile $\bar{\rho}(Z)$ is established by the two-tank method, using fresh water in the first tank and salt water with a density $\bar{\rho} = 1.15$ kg/l in the second tank, leading to a Brunt-Väisälä frequency $N = \sqrt{-(g/\bar{\rho})(\partial\bar{\rho}/\partial Z)}$ close to 2 rad/s.

A circular cylinder of diameter D varying between 0.3 and 1 cm is towed horizontally in the stratified fluid, at a velocity U varying between 0.4 and 4 cm/s. As can be seen on Fig. 1, the cylinder axis is tilted relative to the vertical, at an angle α in the cross-stream plane. A sphere has also been used at large Reynolds number.

The tilted stratified wake of a cylinder is characterized by five non-dimensional parameters: the tilt angle α , the Reynolds number $Re = UD/\nu$, the Froude number $F = U/ND$, the Schmidt number $Sc = \nu/\kappa$ (κ being the diffusivity of salt in water) and the non-dimensional stratification length L . However, the two last parameters

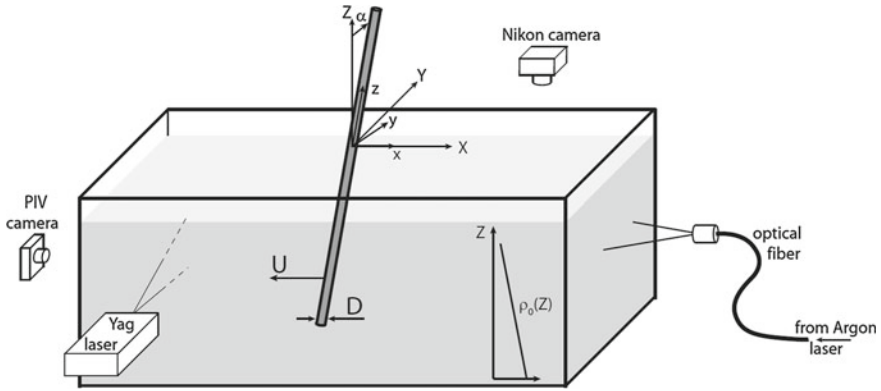


Fig. 1 Schematic of the experimental set-up: the stratified cylinder wake is analyzed by dye visualisations on the *right* side and by PIV measurements on the *left* side

will be assumed very large in this study, which reduces the problem to 3 main non-dimensional parameters.

In order to visualize the flow, a fluorescent dye mixture made of Fluorescein is deposited on the upstream side of the cylinder and then advected in the von Karman vortices. A laser sheet allows to reveal the 2D structure of the flow. Shadowgraph visualisations have also been done by putting a light far from the tank, whose rays are deviated inside the tank (due to the variation of the refractive index with the density) and focused inside a camera on the other side of the tank. This allows to reveal the 3D instabilities of the flow. Finally, Particle Image Velocimetry (PIV) measurements have been obtained by seeding water with small reflecting particles.

3 Two-Dimensional von Karman Vortex Street

It is well known that a cylinder wake exhibits alternate vortices above a critical Reynolds number equal to 49.9 (Williamson 1996b). This von Karman vortex street remain discernible in a turbulent wake at very large Reynolds numbers.

Figure 2 shows dye visualisations behind the cylinder tilted with a 30° angle at a moderate Reynolds number ($Re = 100$). In a homogeneous fluid, it is well known that the wake is unstable at this Reynolds number and leads to a von Karman vortex street. It is indeed what is observed on Fig. 2a because the Froude number is relatively high ($F = 1.8$), i.e. the stratification relatively low.

When the Froude number is decreased to 1.3, the vortex street disappears and is replaced by a stationary recirculation bubble, even though the Reynolds number is still equal to $Re = 100$. This is very clear on the visualisation of Fig.2b, where the dye rolls-up in the two counter-rotating vortices of the recirculation bubble and then stretches in a long straight line with no apparent sinusoidal perturbation.

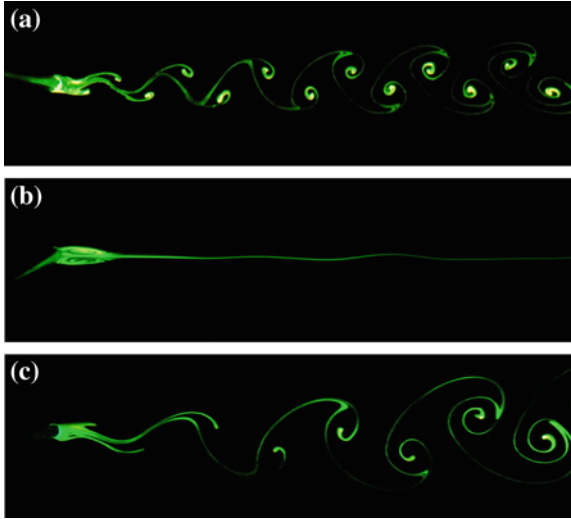


Fig. 2 Dye visualisation of the wake behind a *cylinder tilted* at a 30° angle with respect to the vertical. The pictures are obtained at the same Reynolds number $Re = 100$ and at three different Froude numbers: **a** $F = 1.8$, **b** $F = 1.3$ and **c** $F = 0.8$. The field of view is approximately 35 by 10 diameters in the cross-cut plane (x, y)

Intuitively, the presence of a stratification stabilises the flow because the restoring force tends to attenuate the vertical velocity V created by the tilted vortices (Meunier 2012a, b). This restabilising effect is very similar to the stabilisation of a vertically sheared flow which occurs when the Richardson number is larger than $1/4$, as shown by Miles (1961). Indeed, the von Karman vortex street is generated by the two shear layers which detach from the cylinder and which are subject to a shear instability. This is why the wake is stabilised when the Froude number decreases.

However, it is surprising to see that when the Froude number is decreased further, the wake loses this stability and leads once again to a von Karman vortex street as for a homogeneous fluid. This is clearly shown on Fig. 2c for $F = 0.8$, where the dye rolls up again in the vortices shed on each side of the cylinder. This structure seems to be similar to the von Karman vortex street obtained at high Froude number. However, the wavelength is larger, showing that it is in fact a different unstable mode. Indeed, these vortices do not contain any vertical velocity although their axes are tilted (and parallel to the cylinder), meaning that the streamlines are horizontal ellipses.

This new unstable mode is indicated schematically at low Froude number ($F < 1.3$) in the stability diagram of Fig. 3a. It appears above $Re_c = 45$ at vanishing Froude numbers and at larger Reynolds numbers for larger Froude numbers (up to $Re = 130$). At large Froude numbers, the classical von Karman vortices appear, but they are suppressed by the moderate stratification. These two modes create a strange stability diagram which is more stable only for moderate Froude numbers with a cusp at $F = 1.3$.

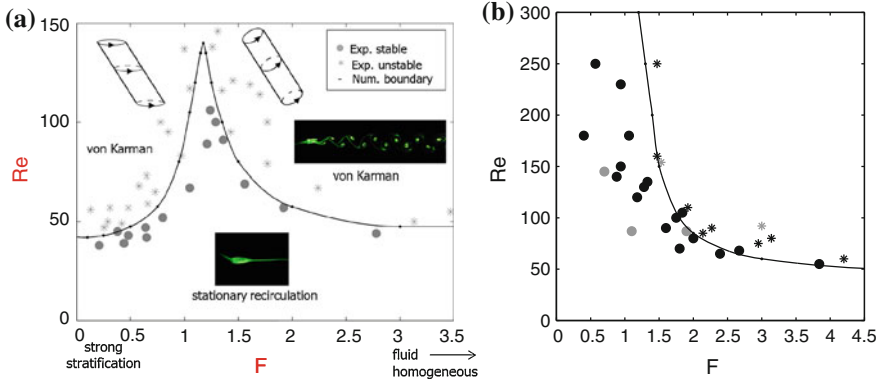


Fig. 3 Stability diagram of the wake of a *cylinder* tilted at **a** $\alpha = 30^\circ$ and **b** $\alpha = 90^\circ$, with respect to the vertical. Symbols correspond to stable (\bullet) and unstable ($*$) experiments. The *solid line* corresponds to numerical results. In **b** *Grey symbols* correspond to the experimental results of (Boyer et al. 1989)

However, when the tilt angle α increases, the low Froude number mode is suppressed because the streamlines become more and more elliptical. The low-Froude part of the critical Reynolds number curve is translated toward smaller Froude numbers and eventually disappears for a horizontal cylinder, as shown in Fig. 3b.

4 Three-Dimensional Instabilities

When the Reynolds number increases, the 2D von Karman vortex street becomes unstable with respect to a 3D instability. This transition has been well studied for a homogeneous cylinder wake, where the first mode (called mode A) exhibits counter-rotating vortex pairs perpendicular to the primary von Karman vortices. They are nicely visualised in Fig. 4 by shadowgraph for a weak stratification. The vortex pairs are clearly visible in the front view. The side view highlights the fact that their tails are advected by the cylinder wake. The wavelength is equal to 4 diameters, as in a homogeneous fluid (Williamson 1996a).

The stability diagram of Fig. 5 indicates that this mode becomes more unstable for moderate stratifications. This is surprising because the mode A is due to the elliptic instability of the von Karman vortices (Thompson et al. 2001), whose growth rate σ decreases with the presence of a stratification as noted by Kerswell (2002):

$$\sigma = \frac{9}{16}\varepsilon\left(1 - \frac{3}{4F_v^2}\right)$$

Here, ε is the ellipticity of the streamlines and $F_v = \Omega(0)/N$ is the vortex Froude number based on the angular velocity at the center of the vortex. We would thus expect

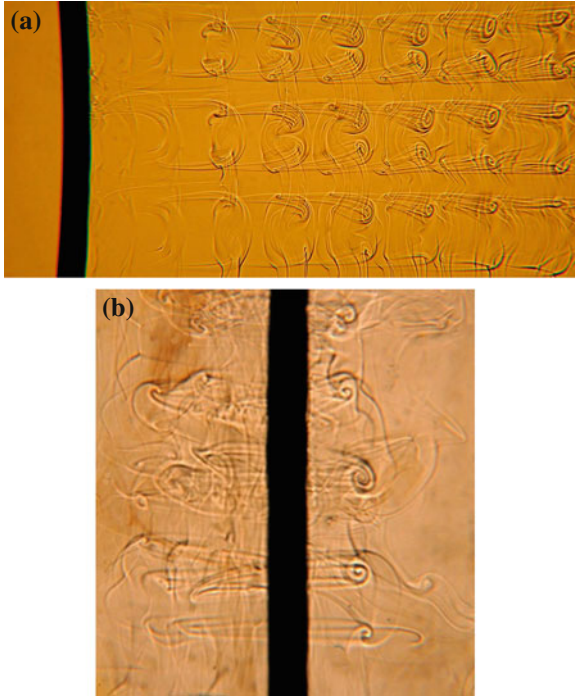


Fig. 4 *Shadowgraph* visualisations of the 3D unstable mode for a *vertical cylinder* ($\alpha = 0^\circ$) in a side view (a) and in a front view (b). $Re = 190$, $F = 4$

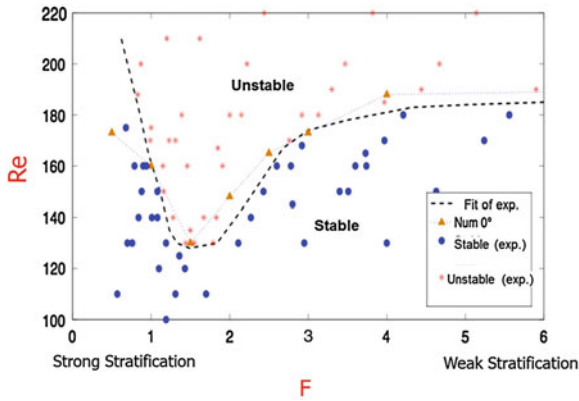


Fig. 5 Stability diagram of the mode A for a *vertical cylinder*

for weak stratification (large F_v) to have a smaller growth rate and thus a larger critical Reynolds number. However, at smaller Froude number ($F < 1.5$), there is a large increase of the critical Reynolds number, probably due to the presence of critical layers in the Kelvin modes of the vortices, as explained by Le Dizès (2008).

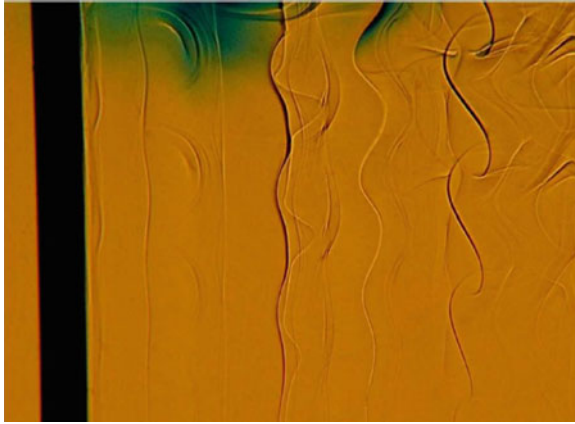


Fig. 6 Shadowgraph visualisations of the 3D unstable mode for a cylinder tilted at $\alpha = 45^\circ$ in a side view. $Re = 180$, $F = 2.5$

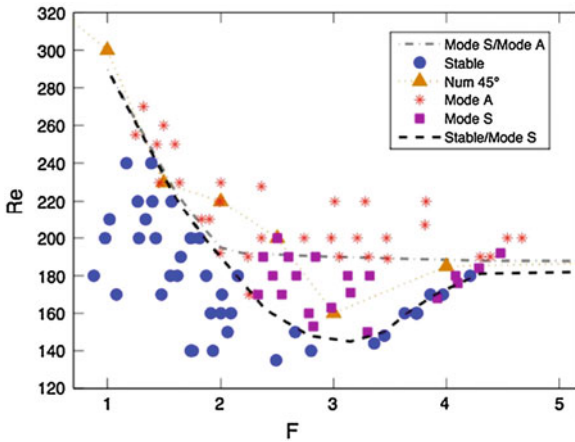


Fig. 7 Stability diagram of the mode S for a cylinder tilted at $\alpha = 45^\circ$

The dynamics of the 3D wake is totally different when the cylinder is tilted with respect to the vertical. Indeed, Fig. 6 shows that thin dark and bright lines appear in the wake, and start to undulate above a critical Reynolds number, creating S shaped lines. This new unstable mode (that we called mode S), only appears for moderate Froude numbers (between 2 and 4), as can be seen in Fig. 7.

At these Froude numbers, the tilted vortices exhibit strong axial flows even in the absence of 3D instabilities. This is clearly visible in the 2D numerical simulations presented in Fig. 8a, where mushrooms of strong positive and negative axial velocity surround the vortices. This characteristic structure can be retrieved theoretically by summing the axial flow created by each vortex, as has been done in Fig. 8b. Indeed,

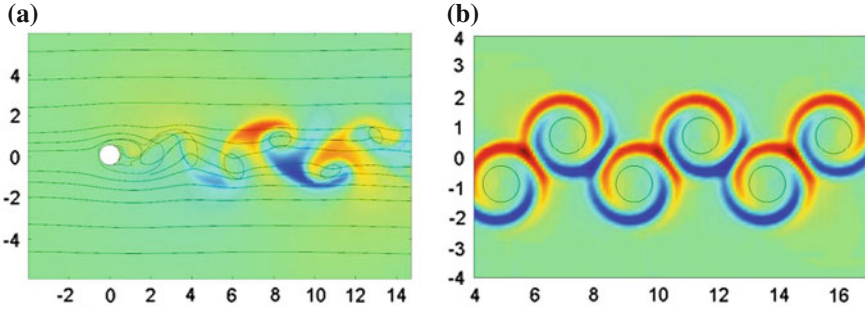


Fig. 8 Axial velocity of the 2D flow generated by the von Karman vortex street (a) numerically and (b) theoretically at $\alpha = 45^\circ$, $F = 2.5$, $\text{Re} = 180$

each tilted vortex contains a critical layer at the radius r_c where the angular velocity $\Omega(r_c)$ is equal to the buoyancy frequency N . This is due to a resonance of the stratified fluid to the periodic vertical forcing at frequency $\Omega(r)$ which is created by the tilted streamlines. At small tilt angle α , Boulanger et al. (2007) showed that the axial velocity is simply equal to

$$w(r) = \frac{r\Omega(r)^3}{\Omega(r)^2 - N^2}$$

and thus diverges at r_c . Inside the critical layer, viscous effects can be taken into account and lead to an analytic solution with an amplitude scaling as $\text{Re}^{1/3}$ and a thickness scaling as $\text{Re}^{-1/3}$. This structure, plotted in Fig. 8, exhibits two embedded positive and negative circular jets. When summing the critical layers of all the von Karman vortices, we recover the mushroom structures found in the exact 2D numerical simulations.

Boulanger et al. (2008) showed that this critical layer creates a strong shear which is unstable with respect to the Kelvin-Helmholtz instability. This is nicely visualised in Fig. 9, where the thin lines start to undulate leading to Kelvin-Helmholtz billows. The lines exhibit an S shape very similar to the structure of the mode S in the wake of the cylinder, which is visualised in Fig. 6. This explains the origin of this new 3D unstable mode of the cylinder wake, due to Kelvin-Helmholtz instabilities of the critical layers.

5 Turbulent Wake

When the Reynolds number increases further, the wake becomes turbulent with the presence of small-scale fluctuations, especially at large Froude numbers. However, the stratification still plays a major role at late stages when the mean velocity of

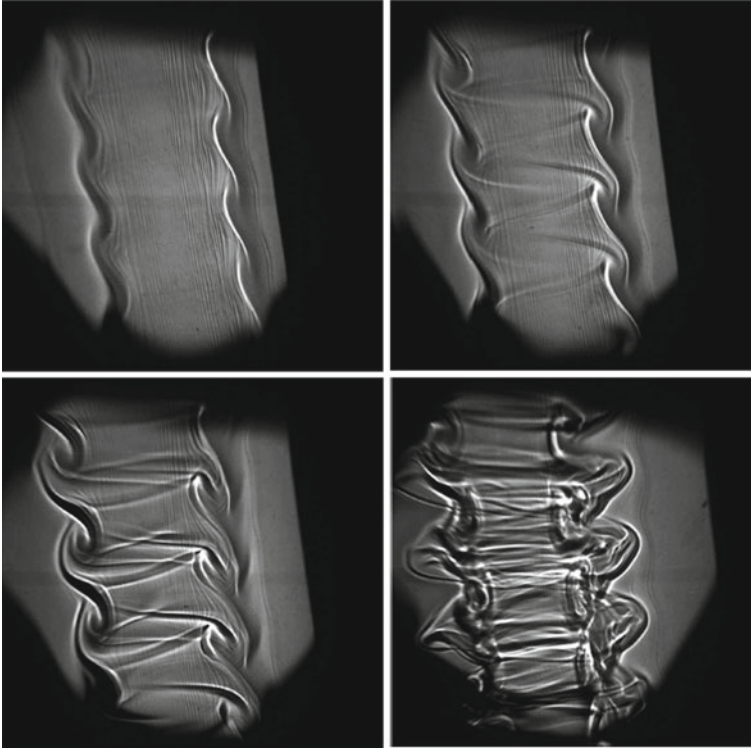


Fig. 9 Temporal development of the tilt-induced instability of a vortex in a stratified fluid tilted at $\alpha = 4^\circ$ visualized by Shadowgraph

the wake has decayed to the characteristic value ND . This leads to the presence of horizontal vortices in order to reduce the vertical velocity, as has been well shown by Lin and Pao (1979) for a sphere wake. The stratification also prevents the extension of the wake in the vertical direction, which imposes a very small aspect ratio of the vortices. As a consequence, the velocity decays slower than in a homogeneous wake because the flow rate is constant.

This can be modeled using a turbulent diffusivity ν_T which depends on time. Indeed, assuming that the Reynolds stresses are proportional to the mean shear, it can be shown that the mean streamwise velocity satisfies a diffusion equation (see Tennekes and Lumley 1972):

$$\frac{\partial u}{\partial t} = \nu_T \left(\frac{\partial^2 u}{\partial y^2} + \frac{\partial^2 u}{\partial z^2} \right) \quad (1)$$

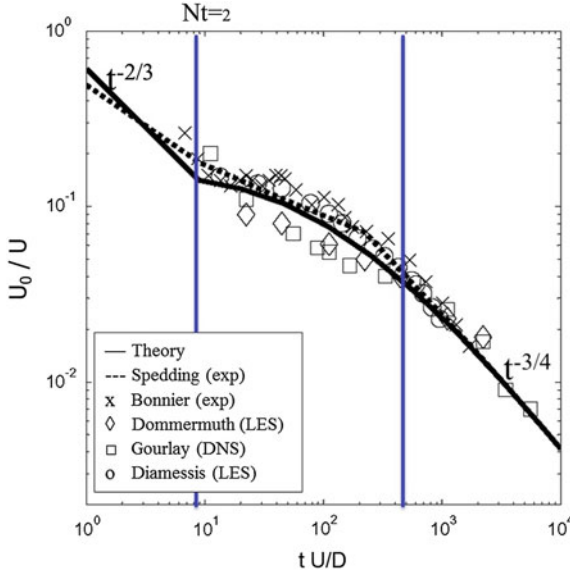


Fig. 10 Mean velocity amplitude of the stratified turbulent wake of a sphere as a function of time

In the homogeneous case, this equation has a Gaussian solution

$$u(y, z, t) = U_0(t) \exp\left(-\frac{y^2}{L_y^2} - \frac{z^2}{L_z^2}\right) \quad (2)$$

with an amplitude $U_0(t)$, a horizontal width $L_y(t)$ and a vertical height $L_z(t)$ which depend on time. If the turbulent diffusivity ν_T is proportional to $U_0 L_y$, the amplitude decreases as $t^{-2/3}$ and the width and height increase as $t^{1/3}$. This is indeed observed in homogeneous wakes and in the early stages of stratified wakes, as shown on Fig. 10 for $Nt < 2$. However, at $Nt \sim 1$, the amplitude U_0 becomes close to NL_y and the wake starts to feel the effect of the stratification. The turbulent vertical velocities are suppressed such that the vertical Reynolds stress $\langle u'w' \rangle$ vanishes. The turbulent diffusive term $\nu_T \partial^2 u / \partial z^2$ must be replaced by a viscous diffusive term $\nu \partial^2 u / \partial z^2$, which is much smaller (Meunier et al. 2006). This explains why the mean profile expands in the horizontal direction but not in the vertical direction. The amplitude U_0 decreases as $t^{-1/2}$ like in a 2D homogeneous wake, leading to a slower decay of the wake. This is clearly visible in Fig. 10 for $Nt > 2$, where the initial decay is drastically slowed down when the stratified effects become important.

However, at very late stages, the viscous diffusion eventually becomes important and leads to an extension of the wake in the vertical direction. This creates a decrease as $t^{-3/4}$ of the amplitude of the wake U_0 . This is visible in Fig. 10 for $Nt > 50$ and has been called the quasi-2D regime in the literature (Spedding 1997).

Taking the empirical values of the coefficients between the Reynolds stress and the mean shear, it is possible to predict the exact laws for the velocity amplitude with no fitting parameter. This is plotted in Fig. 10 and compared to all the experimental and numerical data found in the literature. There is an excellent agreement, which indicates that a simple model of turbulent diffusivity can accurately predict the mean characteristics of a stratified wake.

6 Conclusion

This chapter highlights the fact that a density stratification such as the stratification of the atmosphere or the oceans can drastically modify the structure and dynamics of a bluff body wake. At small Reynolds numbers, the transition from a stationary wake to a 2D time-periodic and then to a 3D wake are highly dependent on the Froude number and on the orientation of the bluff body, which gives a very rich dynamics of bifurcations and instabilities. At large Reynolds numbers, the stratification plays a major role in the late stages even for a weak stratification.

All these results indicate that a great care should be taken when using simple models of homogeneous wakes for geophysical applications of mountain or island wakes. The presence of resonances and waves creates a very complex and surprising structure of the wake, which has been very weakly studied in clean laboratory experiments or even in numerical simulations. How are modified the transitions for different bluff bodies? What is the structure and stability of the lee waves for a 3D bluff body? How much mixing is created by these 3D wakes? These are a few questions that will need to be answered for a better understanding and modeling of geophysical wakes.

Acknowledgments Special acknowledgements to Prof. Anne Cros for her invitation to the congress of the División de Dinámica de Fluidos. I also thank the Secretaría de Relaciones Exteriores, Dirección General de Cooperación Educativa y Cultural de México for their financial support. Finally, I would like to thank Prof. Geoff Spedding for introducing me to the study of stratified wakes.

References

- Boulanger N, Meunier P, Le Dizès S (2007) Structure of a stratified tilted vortex. *J Fluid Mech* 583:443–458
- Boulanger N, Meunier P, Le Dizès S (2008) Tilt-induced instability of a stratified vortex. *J Fluid Mech* 596:1–20
- Boyer DL, Davies PA, Fernando HJS, Zhang X (1989) Linearly stratified flow past a horizontal circular cylinder. *Philos Trans R Soc Lond Ser A* 328:501
- Le Dizès S (2008) Inviscid waves on a lamb-oseen vortex in a rotating stratified fluid: consequences for the elliptic instability. *J Fluid Mech* 597:283
- Kerswell RR (2002) Elliptical instability. *Ann Rev Fluid Mech* 34:83–113

- Lin JT, Pao YH (1979) Wakes in stratified fluids: a review. *Ann Rev Fluid Mech* 11:317–338
- Meunier P (2012a) Stratified wake of a tilted cylinder. Part 1. Suppression of a von Karman vortex street. *J Fluid Mech* 699:174–197
- Meunier P (2012b) Stratified wake of a tilted cylinder. Part 2. Lee internal waves. *J Fluid Mech* 699:198–215
- Meunier P, Diamessis P, Spedding GR (2006) Self-preservation in stratified momentum wakes. *Phys Fluids* 18:106601
- Miles JW (1961) On the stability of heterogeneous shear flows. *J Fluid Mech* 10(4):496–508
- Spedding GR (1997) The evolution of initially turbulent bluff-body wakes at high internal Froude number. *J Fluid Mech* 337:283–301
- Tennekes H, Lumley JL (1972) *A first course in turbulence*. M.I.T Press, Cambridge
- Thompson M, Leweke T, Williamson C (2001) The physics mechanism of transition in bluff body wakes. *J Fluids Struct* 15:607
- Williamson CHK (1996a) Three-dimensional wake transition. *J Fluid Mech* 328:345–407
- Williamson CHK (1996b) Vortex dynamics in the cylinder wake. *Ann Rev Fluid Mech* 28:477–539